6 Nonclinical Imaging Studies for the Diagnosis of Lymph Node Metastases

Kazunobu Ohnuki and Hirofumi Fujii

Abstract

Nonclinical studies using animal models are essential to elucidate the pathogenesis of lymph node metastases and the application of imaging tests in this research field is very important because these tests can yield reliable results at the sacrifice of minimal number of animals.

Animal models and imaging modalities must be carefully selected to obtain fruitful results. Recently, imaging devices dedicated for small animal tests have been developed for various kinds of imaging modalities including combined scanners and they have contributed to the improvement of the quality of images of metastatic lesions in lymph nodes.

In the imaging study of lymph node metastases, direct detection of metastatic foci in lymph nodes is ideal. But, it is often difficult because early stages of metastatic lesions are too small to depict. Sentinel node mapping is an alternative way to diagnose small metastatic lesions in regional lymph nodes. Since new imaging modalities including optical imaging are recently proposed to identify sentinel nodes, nonclinical animal experiments to investigate these new imaging tests are attracting attentions of researchers.

Another idea to detect small metastatic foci is to observe the change in non-tumor areas of metastatic lymph nodes. As recent animal models can simulate tumor microenvironments in human tumors well, visualization of functional information inside lymph nodes such as immunological response in sentinel nodes is expected.

Keywords

Lymph node metastases · Small animal imaging · Dedicated scanner Sentinel node

K. Ohnuki · H. Fujii (✉)
Division of Functional Imaging, Exploratory Oncology Research and Clinical Trial Center (EPOC), National Cancer Center, Kashiwa, Japan
e-mail: fujii-rad@umin.org

S. Natsugoe (ed.), *Lymph Node Metastasis in Gastrointestinal Cancer*,
https://doi.org/10.1007/978-981-10-4699-5_6

6.1 Introduction

Nonclinical studies using animal models play an important role to elucidate the pathogenesis of various kinds of disease including cancer. As for the investigation of lymph node (LN) metastases of malignant tumors, animal experiments are useful to develop methods to evaluate lymphatic flow from tumor foci and to evaluate metabolic changes inside metastatic nodes. When a good candidate of a new tracer for sentinel node (SN) mapping is successfully developed, preclinical studies to evaluate its biodistribution and toxicity are essential before starting its clinical trial.

An in vivo imaging test can provide biological information in living bodies. It is very important in biological studies because it is doubtful whether the information obtained from conventional postmortem studies can correctly express the activities inside living animals or not. Recent advance in veterinary science such as gene recombination has also enabled researchers to reproduce almost natural environments in animal models. The investigation of immune response is extremely important in researches about metastases of cancer. Now, we can have animal models with human tumor xenografts whose immune system is almost natural [1]. Under such conditions, immunological response in metastatic nodes might be experimentally evaluated.

When animal experiments are performed, it is very important to derive reliable and meaningful results from the least number of animals in the light of animal welfare. Researchers can observe the longitudinal change of same animals by examining them using in vivo imaging tests. As a result, the total number of sacrificed animals can be minimized in in vivo imaging studies because researchers do not have to dissect animals at each time point of the study. Moreover, in vivo imaging tests can enhance the preciseness of investigations because interindividual errors would be minimized by longitudinally observing same animals.

Considering these merits, the usefulness of in vivo imaging tests would be immeasurable. In this chapter, we introduce current in vivo imaging tests that are applicable to animal experiments such as computed tomography (CT), magnetic resonance imaging (MRI), nuclear medicine tests, ultrasonography (US) tests, and optical imaging tests. Recently, many kinds of imaging devices dedicated for small animal tests have been developed. The features of scanners for small animals are also mentioned. After that, we describe the usefulness of these in vivo imaging tests in researches of LN metastases [2].

6.2 Animal Models for Studies with Lymph Node Metastases

6.2.1 Types of Animal Models

Animal models that are used in experimental oncology studies are roughly classified into the following three groups: (1) transplantation models, (2) carcinogen-induced models, and (3) genetically modified models including transgenic models

Table 6.1 Classifications of preclinical animal models

Category	Characterization (description)	Advantages	Disadvantages
Transplantation models	1. The most commonly used animal models 2. Transplantation of cancer cell lines or xenografts into wild-type or immunocompetent inbred animals	1. Simple procedure and easy tumor monitoring 2. Easy-to-use (rapid assessment, reproducible and low cost)	1. Considered "poorly realistic" for multiple reasons 2. Genetically homogeneous tumor development lacks many features of spontaneously occurred tumors.
Carcinogen-induced models	1. Induced by carcinogens such as UV light and DNA-damaging agents such as DMBA and TPA	1. More realistic features such as diversity and high heterogeneity 2. Normal immune system	1. Long time to obtain 2. Difficulties in continuous tumor monitoring 3. Absence of defined genetic manipulation
Genetically modified model	1. Transgenic expression of oncogenes or the inactivation of tumor suppressor genes 2. Bring in important insights into the relationship between cancer and the immune system.	1. Accurately reflect features of human diseases 2. Yield useful insights into the interaction between malignant cells and immune effectors	1. Long time to obtain 2. Features of tumors depend on the strain of host animals. 3. Difficulties in continuous tumor monitoring 4. High cost

Modified with permission from Table 1 in Ref. [1]

[1]. Each model has both advantage and disadvantage and these are summarized in Table 6.1.

Since most commonly used in studies about LN metastases are transplantation models among them, we mainly describe this types of models in this chapter.

Transplantation models can be sub-classified from two kinds of viewpoints. In the light of the relationship between host and transplantation cells, these models can be classified into syngeneic ones and xenograft ones. In the light of transplantation sites, transplantation models can be classified into orthotropic ones and ectopic ones. The features of these models are summarized in Table 6.2.

Some animal models that are used for experiments of LN metastases are reported in mice, rats, swine, and so on. Among them, mouse models are most popular. Mouse models are generally easy to handle and there are many immunocompromised models.

Xenograft-orthotopic models and syngeneic-orthotopic models are common and some syngeneic-ectopic (mainly subcutaneous transplantation) models are also reported. Representative animal models with LN metastases are shown in Table 6.3.

When human tumor cells are examined, xenograft models whose hosts are (1) BALB/c $^{nu/nu}$ mice that are most popular nude mice, (2) severe combined immunodeficiency (SCID) ones, and (3) nonobese diabetic (NOD)/SCID ones are

Table 6.2 Classifications of tumor transplantation models

	Category	Advantages	Disadvantages
The original species	Synergic	1. Normal immune system in host animals 2. Easy-to-use (rapid assessment, reproducible and low cost)	Hard to evaluate human tumors
	Xenograft	1. Use tumor cells obtained from actual patients. Recently, patient-derived xenograft (PDX) models are actively investigated.	Expensive host animals
The transplantation sites	Orthotopic	Investigation of original features of tumor cells including tumor microenvironments would be expected.	1. High cost 2. Difficulties in tumor monitoring 3. Difficult to evaluate the tumor initiation. 4. Limited metastatic ability
	Ectopic	Transplantation site can be chosen according to the purpose of studies. The interval changes of size would be easy in subcutaneous models.	The features of tumors might be different from original ones.

Modified with permission from Ref. [3]

Table 6.3 Animal models with lymph node metastases

Mouse models					
Syngeneic-Orthotopic models					
Tumor type	Cell line	Host	Inoculation site	Lymph nodes of interest	Refs.
Colon cancer	CT26	BALB/c	Submucosal layer of the cecal wall	Mesenteric LNs	[4]
Pancreatic cancer	Pan02 6606PDA	C57BL/6	Head or tail of the pancreas	Mesenteric and peritoneal LNs	[5, 6]
Bladder tumor	MBT-2	C3H	Bladder epithelial layer	Iliac LN	[7]
Breast cancer	4T1	BALB/c	Mammary fat pad	Axillary and inguinal LNs	[8, 9]
Melanoma	B16 [F0, F1, F10]	C57BL/6	Subcutaneous	Inguinal LN	[10, 11]
Xenograft-Orthotopic models					
Gastric cancer	SGC-7901	BALB/c nu/nu	Implanted in the gastric wall (2 mm diameter pieces)	Mesenteric LNs	[12]
	OCUM-2MLN	BALB/c nude	The stomach wall of the antrum ($2 \times 10^6 - 1 \times 10^7$)	Regional LNs	[13]

Table 6.3 (continued)

	44As3, 58As1, 58As9 (Derived from HSC-44PE, HSC-58)	BALB/c nude	Implanted in the middle wall of the greater curvature of the stomach (2×10^6)	Regional LNs	[14]
Colorectal cancer	HT-29 HCT116	BALB/c nu/nu	Implanted in the cecal wall between the mucosa and the muscularis externa layers (2×10^6)	Peripancreatic, axillary and inguinal LNs	[15]
	HT-29 HCT116	CB17 SCID	1 mm^3-sized fragment implanted in the cecal wall	Regional LNs	[16]
	LS174T, HT-29	CB17 SCID	Techniques of transanal low-dose colonic mucosal electrocoagulation (1×10^6)	Mesenteric and retroperitoneal LNs	[17]
Esophageal cancer	PT1590	NMRI/nu	1 mm^3-sized fragment implanted in the abdominal esophagus	Mesenteric, coeliac, paraesophageal and axillary LN	[18]
Breast cancer	MDA-MB -231	BALB/c nu/nu	Mammary fat pad	Axillary and inguinal LN	[19]
Rat models					
Tumor type	Cell line	Host	Inoculation site	Lymph nodes of interest	Refs.
Liver hepatoma	AH130	Donryu rats	Cecum submucosa	Meso-cecum LNs	[20]
Hepatocarcinoma	He/De	Buffalo rat	Capsule of the left kidney	Parathymic LNs	[21]
Other animal models					
Animal	Cell line	Host	Inoculation site	Lymph nodes of interest	Refs.
Rabbit	VX2 squamous cell carcinoma	New Zealand white rabbits	Submucosal layer of the stomach	Intraperitoneal LN	[22]
Rabbit	VX2 squamous cell carcinoma	New Zealand white rabbits	The submucosa of the lateral wall of the pyriform sinus.	Parotid LN	[23]
Swine	(Melanoma)	Sinclair miniature swine	(Spontaneous)	Regional draining LNs	[24]
Swine	(Melanoma)	Sinclair miniature swine	(Spontaneous)	LN in the posterior neck	[25]

commonly used. Among xenograft models, orthotopic ones are recently getting popular because the interaction between tumor cells and stromal cells is attracting attention of researchers.

Cancer immunotherapies including immune checkpoint molecules such as programmed cell death-1 ligand-1 (PD-L1), programmed cell death-1 (PD-1), and cytotoxic T-lymphocyte antigen-4 (CTLA-4) are current topics. Since animal models used in researches in this field must have normal immune system, syngeneic models with normal immune system must be selected instead of immunocompromised xenograft models. A recent study reported that transplantation of human hematopoietic stem cells into NOG (NOD/Shi-*scid*, IL-2Rγ^{null}) [26] or NSG (NOD-*scid* IL2Rγ^{null}) [27] mice can simulate human immune system to some degree.

The optimal models should be selected considering the aim of researches and this is very important to investigate the pathogenesis [28].

6.2.2 The Production of Transplantation Model for Experiments of LN Metastases

When transplantation models with LN metastases are produced by injecting tumor cells in tissues, researchers must carefully inject tumor cells with minimal pressure. When cancer cells are injected in soft tissues of footpads of mice putting pressure, the pressure in tissues increases and gaps between endothelial cells of lymph channels are enlarged [29]. As a result, cancer cells can easily migrate into lymphatic vessels and move into popliteal LNs, which correspond to SNs of footpads, on nonphysiological lymphatic flow. Then, unexpected metastatic lesions can appear inside popliteal LNs.

Lymphatic flow is an important factor in experiments to identify SNs and evaluate the location of metastatic foci inside SNs [30]. When the results of experiments are sensitive to the conditions of lymphatic flow, tumor cells and/or SN-seeking probes should be slowly injected using injecting devices (Fig. 6.1).

6.3 Imaging Tests for Animal Models with Lymph Node Metastases

6.3.1 Computed Tomography (CT) Tests

In X-ray computed tomography tests, the object is irradiated from multiple directions, and X-ray signals that penetrated the object are acquired by X-ray detectors. The acquired X-ray signals are mathematically reconstructed and tomographic images of the object are obtained. CT images can provide minute anatomical information and this test is the most basic and important imaging test.

Recently, X-ray CT scanners dedicated for small animals are developed (Fig. 6.2).

Its spatial resolution is very excellent and it is usually less than 0.1 mm. But, the tissue contrast of CT images is not so good. As CT numbers of tumors and parenchymal organs are similar, it is not easy to distinguish tumors from normal

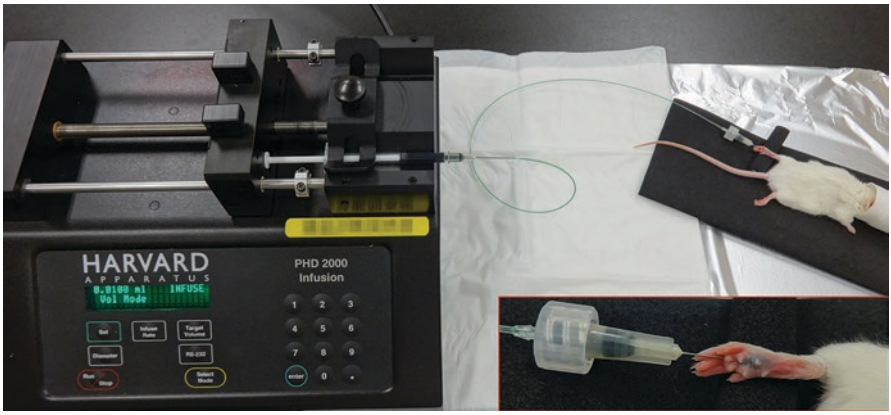

Fig. 6.1 Slow injection with constant speed by a syringe pump (Harvard Apparatus, Holliston, MA, USA)

Fig. 6.2 Preclinical CT imaging system (Latheta LCT-200; Hitachi, Tokyo, Japan)

parenchymal organs on CT images. Since CT numbers of fat and parenchymal organs are different, tumors can be depicted when they are surrounded by fat tissues. But, fat deposition between organs is not prominent in rodents and it is not easy to interpret CT images of small animals. LNs are usually depicted as small soft tissue nodules in fat tissues on CT images (Fig. 6.3).

Fig. 6.3 A normal popliteal LN of a mouse in the CT image (arrow)

Contrast media including iodine compounds for small animal CT tests are now commercially available as clinical CT tests. Contrast media can contribute the diagnosis of tumors because tumors are often rich in vasculature.

6.3.2 Nuclear Medicine Tests

In nuclear medicine tests, radioactive compounds that emit gamma rays or X-rays are administered in living bodies and the biodistribution of administered agents are imaged by acquiring emitted photons by detectors, which is usually made of scintillators such as sodium iodine. But, recently, semiconductor detectors are also used.

Nuclear medicine tests are classified into two categories: (1) conventional nuclear medicine tests in which single photon emitters such as ^{99m}Tc and ^{111}In are used and (2) positron emission tomography (PET) in which positron emitters such as ^{18}F are used. Recently, dedicated scanners for small animal imaging are commercially available for both nuclear medicine tests.

In conventional nuclear medicine tests of small animal imaging, tomographic imaging called single photon emitted computed tomography (SPECT) is usually performed. The performance of SPECT scanner strongly depends on that of collimators. In clinical SPECT scanners, parallel-hole collimators are usually equipped to get good sensitivity. But, the spatial resolution of parallel-hole collimators is bad. Since the size of the object is much smaller than human bodies in small animal imaging, both excellent spatial resolution and good sensitivity, which are generally trade-off, are required in small animal imaging. To overcome this trade-off issue, unique multi-pinhole collimators are used in small animal SPECT scanners (Fig. 6.4).

Scanners with multi-pinhole collimators can show excellent spatial resolution as short as 1 mm and good sensitivity of approximately 0.1% for ^{99m}Tc [31].

In PET scanners, annihilation gamma rays produced by the collision of positron and regular electron are acquired by coincidence detectors. This detection system

Fig. 6.4 A multi-pinhole collimator for small animal SPECT imaging

enables to omit collimators from scanners and PET scanners show rather better sensitivity (>1%) than SPECT scanners.

Although both kinds of nuclear medicine tests can provide meaningful functional information of the object animals, locations where interesting reactions occur are often unclear because nuclear medicine tests can provide no anatomical information. To overcome this issue, combined scanners of nuclear medicine ones and morphological imaging ones are developed for animal imaging (Fig. 6.5).

When radiopharmaceuticals accumulate in LNs, the LNs are drawn as hot spots. SN mapping using radiocolloids is performed based on this concept. The details of this test are described in the latter section.

6.3.3 Magnetic Resonance Imaging (MRI) Tests

MRI is an imaging test in which signals induced by nuclear magnetic resonance (NMR) phenomena are visualized. When the objects are put in high magnetic fields and electric waves with special frequency are irradiated, tissue-specific signals are emitted based on NMR phenomena. MR images can be obtained by acquiring these NMR signals and mathematically reconstructing them. By changing the strength of magnetic fields and the patterns of irradiating electric waves, which is called pulse sequence, images with various kinds of tissue contrast are available. The most

Fig. 6.5 A SPECT/CT combined scanner (NanoSPECT/CT, Mediso, Budapest, Hungary)

important parameters to acquire images are repetition time (TR) and echo time (TE). By changing these two imaging parameters, various kinds of images are available. The representative images are T1-weighted image (T1WI) and T2-weighted image (T2WI).

Normal tissues show intermediate signals on both T1WIs and T2WIs (Fig. 6.6).

Compared to normal tissues, tumor lesions usually show lower signals on T1WIs and higher signals on T2WIs.

Contrast media including paramagnetic agents such as gadolinium and iron are used to enhance the contrast between tissues.

MRI tests can provide detailed anatomical information with good tissue contrast. Spatial resolution can reach less than 0.1 mm. Moreover, MRI tests can also present unique functional information about temperature, pH, and so on by modifying pulse sequences of electric waves.

Some scanners dedicated for small animal imaging are developed for MRI, too. As the diameter of the bore can be short for these animal imaging scanners, compact scanners with high magnetic fields can be manufactured (Fig. 6.7).

In MRI, image quality can be improved by using receiver coils that can be set near the target sites. When special receiver coils that fit bodies of small animals such as rodents are introduced, images of small animals with good quality can be obtained even when clinical scanners with large bores are used [32].

Fig. 6.6 A normal popliteal LN of a mouse on the T2WI MR image obtained by a 3.0T scanner (arrow)

Fig. 6.7 A preclinical 9.4T MR scanner (BioSpec, BRUKER, Etlingen, Germany)

6.3.4 Optical Imaging

Optical imaging is now attracting interests of researchers in the field of molecular imaging because optical imaging devices are usually more compact than other imaging devices such as CT scanners and MRI scanners and it is easy for researchers in biological fields to operate optical imaging devices (Fig. 6.8).

In optical imaging, signals from living bodies are acquired by detectors dedicated for light signals such as charge coupled device (CCD) detectors and complementary metal oxide semiconductor (CMOS) detectors. Optical agents are often administered to the animals before imaging. Previously, signals of only visual lights were observed. But, recently, optical technology has advanced and optical signals with wide range of wave lengths can be acquired. Especially, imaging of

Fig. 6.8 An in vivo optical imaging system (IVIS® Spectrum, PerkinElmer, Waltham, MA, USA)

near-infrared light signals, whose wave length is longer than 800 nm and which are invisible to human eyes, is actively investigated because little background signals are detected from living bodies in the range of wave length of near-infrared lights. That is why this range of wave length is called "biological windows." When optical imaging agents that emit fluorescent lights with this range of wave length are administered, the biodistribution of imaging agents can be depicted with good contrast to background areas of normal tissues.

Indocyanine green (ICG, Daiichi-Sankyo, Tokyo), which is a blue dye that is used for SN mapping, also emits near-infrared fluorescent signals. As this dye has already been used in routine clinical practice under the coverage of health insurance in Japan, near-infrared light imaging using this dye are investigated in many institutes (Fig. 6.9).

6.3.5 Ultrasonography (US)

US is an imaging test in which the behavior of high-frequency sound waves inside living bodies is observed. High-frequency sound waves produced by piezoelectric transducers are transmitted to the objects. Some sound waves in the objects are reflected from the layers between different tissues and some of these echoes are detected as signals. The obtained echo signals are reconstructed into images. As US imaging devices are usually compact and some devices are portable, US tests can be easily performed in regular experimental rooms (Fig. 6.10) [33].

The depth to which sound waves can reach depends on the frequency of sound waves and structure of the objects. Sound waves with high frequency can visualize the minute structure of tissues while they cannot reach deep areas. There is the trade-off between image resolution and observable depth. In small animal imaging, sound waves whose frequency was 10–50 MHz were used to visualize minute structure in small objects. Although the depth that can be observed would be limited to a few centimeters, LNs located in the superficial area can be clearly detected by US [34] (Fig. 6.11).

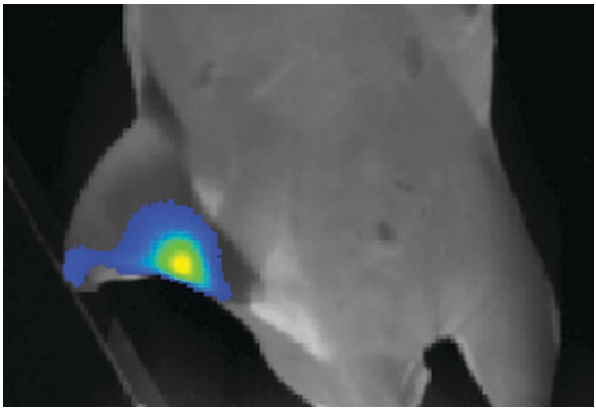

Fig. 6.9 A SN in the popliteal region of a mouse visualized by near-infrared fluorescent signal. The image was obtained after the subcutaneous injection of the ICG in the left footpad by an in vivo optical imaging system

Fig. 6.10 A high-frequency ultrasound imaging system (Vevo® 3100, FUJIFILM Visualsonics, Inc.; Toronto, Canada)

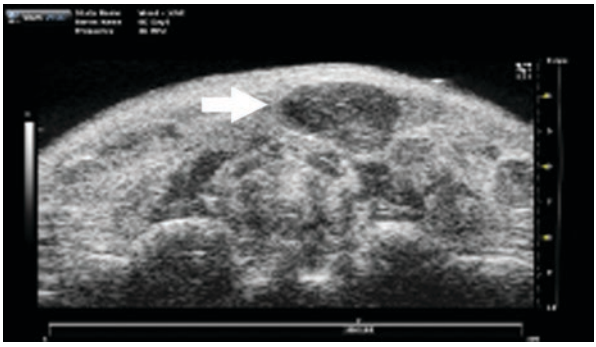

Fig. 6.11 A normal superficial cervical LN of a mouse in the ultrasound image (arrow). Reprinted with some modification with permission from Ref. [34]

There are some contrast media for US, too. Most of contrast media for US are microbubble agents made of phospholipids or carbohydrates. When these agents are administered and accumulated in the target tissues, echo signals on US images are enhanced by the increase of the reflection of sound waves.

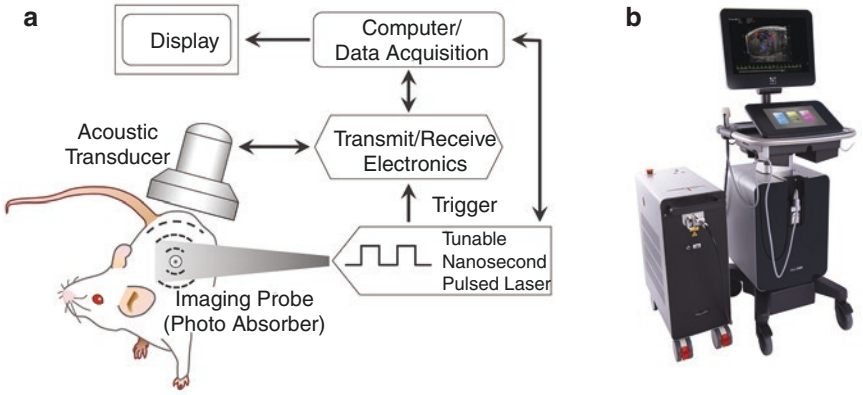

Fig. 6.12 Photoacoustic imaging (PAI) system. (**a**) Schematic diagram of PAI system. (**b**) The Vevo® LAZR Photoacoustic Imaging System (FUJIFILM Visualsonics, Inc.; Toronto, Canada)

6.3.6 Opt-acoustic (Photoacoustic) Imaging

Opt-acoustic or photoacoustic imaging is a new imaging modality although the mechanism of this imaging modality was first reported by Alexander Graham Bell, who is famous for the invention of telephone, in 1880 [35].

When light signals are delivered into the tissues, some energy of light signals is converted into heat and, finally, photoacoustic waves are induced. These phenomena are called photoacoustic effects and sound waves induced by these effects can be detected by US scanners [36] (Fig. 6.12).

According to the review article by James ML and Gambhir SS [33], opt-acoustic imaging tests have the following advantage compared with the conventional US tests: (1) the amount of imaging agent used for opt-acoustic imaging is picograms to micrograms, whereas US requires microgram to milligram amounts of imaging agent; and (2) US images contain speckles (noise) due to coherent addition of sound waves. In the case of "light in and sound out, opt-acoustic imaging" there is very minimal interference for the sound waves on their way out; therefore, the images are speckle free.

6.4 Direct Visualization of LN Metastases

6.4.1 Computed Tomography (CT)

When LNs are involved by metastatic lesions, the size of LNs increase and their shape changes to round sphere from flat ellipsoid according to the growth of metastatic lesions. CT tests can detect these morphological changes. Among them, the enlargement of the short axis of LNs can be usually the most important finding to diagnose LN metastasis. There are many reports about the size criteria on LN

Fig. 6.13 A metastatic popliteal LN in the CT image (arrow), which is swollen compared to the contralateral one

metastases in human CT tests. For example, Dorfman, et al. reported that the normal upper limit of LN size in human upper abdomen would be 6–11 mm in human CT studies [37].

But, there are little reports about the size criteria on LN metastases in animal CT tests. As for animal studies, it would be useful to compare the size of affected LN with that of the LN on the opposite side (Fig. 6.13).

As described above, these morphological changes can occur when metastatic lesions in LNs grew to some size. It is difficult to detect early stage of metastases by CT tests.

When contrast media are administered, metastatic LNs are likely to be more strongly enhanced than normal LNs. This finding on CT tests with contrast media might improve the accuracy in the diagnosis of LN metastases. But, it is not easy to detect small LN metastases even by contrast-enhanced CT tests.

There are some other pitfalls in the diagnosis of LN metastasis by CT tests. One of the most important pitfalls is the enlargement of LNs due to inflammation. Inflamed LN can be also enlarged and round-shaped.

6.4.2 Nuclear Medicine Tests

In nuclear medicine tests, LN metastasis can be diagnosed by evaluating the functional information in LNs. The most popular nuclear medicine test to diagnose malignant tumors is ^{18}F-fluorodeoxyglucose (FDG) PET test. This test can evaluate the activity of glucose metabolism in lesions. Glucose metabolism in LNs is usually activated when LNs are involved by tumors. Therefore, metastatic LNs show high avidity to FDG and they are visualized as hot spots on FDG PET images [38](Fig. 6.14).

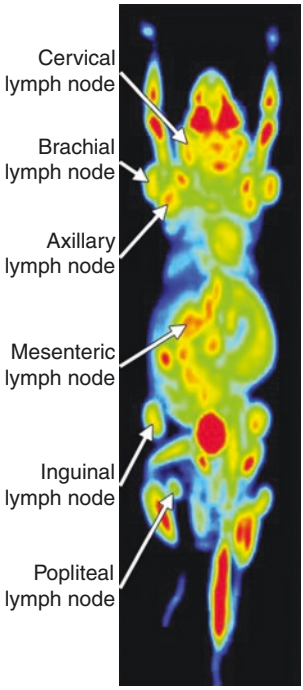

Fig. 6.14 LN metastases of plasma cell tumor-bearing mouse in ^{18}F-FDG-PET image. Reprinted with some modification with permission from Ref. [38]

FDG PET tests have the potential to detect metastatic LNs with normal size by the increased activity of glucose metabolism. But, it is impossible to detect small metastatic LNs even by FDG PET tests, too. Inflammatory lesions in LNs can also be false-positive findings in FDG PET tests because some kinds of cells inside inflamed LNs such as activated macrophages show high avidity to FDG.

The activation of glucose metabolism is a common finding in malignant lesions. As a finding more specific to lymph node metastasis, lymphangiogenesis in LNs, which is considered as an early sign of LN metastasis, is attracting attention of researchers. Lymphatic vessel endothelial hyaluronan receptor 1 (LYVE-1) is a lymphatic-specific epitope and it is expected to be a biomarker of lymphangiogenesis (Fig. 6.15). Mumprecht et al. [39] reported that immuno-PET using ^{124}I-labled LYVE-1 successfully detected early stage of LN metastasis in mouse experiments.

6.4.3 Magnetic Resonance Imaging (MRI) Tests

Metastatic LNs are imaged as enlarged LNs in MR tests as shown in CT ones. In addition to these morphological changes, MRI can provide more detailed information about interiors of metastatic LNs than CT. The most common MR images are T1WIs and T2WIs on spine echo sequences. Generally speaking, tumor lesions show lower signal on T1WI and higher signal on T2WI, compared with normal LNs. Complicated interiors of LNs including metastatic foci cause heterogeneous signal pattern on MR images (Fig. 6.16).

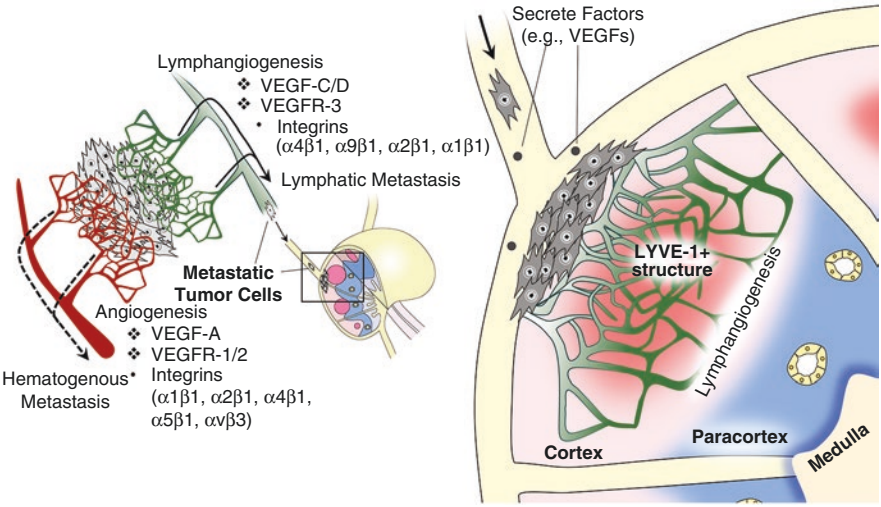

Fig. 6.15 The theory to visualize metastatic LNs by targeting lymphangiogenesis. The lymphatic vessels induced in SLN are composed of LYVE-1-positive lymphatic endothelia, which are expected to be the target of the anti-LYVE-1 antibody

Fig. 6.16 A metastatic popliteal LN of a Balb/c mouse inoculated with Colon26 tumor cells in the T2W MR image (arrow)

Heterogeneous signal patterns can be more significant on MR images obtained by scanners with strong magnetic field such as 9.4T. Administration of contrast media including paramagnetic agents can also enhance the contrast between tumors and non-affected areas. Contrast media can shorten both T1 and T2 relaxation times. When the concentration of contrast media is low, T1 relaxation time is prominently shortened. On the contrary, when the concentration of contrast media is high, T2 relaxation time is strongly shortened. In the diagnosis of LN metastases, contrast-enhanced T1WIs with Gd-chelating agents are usually acquired utilizing the T1 shortening effect. Metastatic lesions in LNs are brightly depicted on these images.

Inflammatory changes and fat deposits in LNs can cause false-positive findings.

6.4.4 Optical Imaging

In optical imaging, optical signals can be detected from metastatic LNs when optical agents that show high affinity to tumor tissues are administered. Unfortunately, no good optical imaging agents to visualize wide variety of tumors like FDG in PET tests. One of the popular optical imaging methods to visualize metastatic LNs is to use tumor-seeking agents conjugated with IRDye 800 CW, a fluorescent dye that emits near-infrared lights with the wave length of 800 nm [40] (Fig. 6.17).

In animal experiments with transplantation models, bioluminescence imaging is also available to investigate LN metastases. When tumor cells with luciferase activity are implanted to animals, tumor lesions can emit luminescent lights. When these tumor cells metastasized to LNs, these LNs with metastatic lesions are also visualized by bioluminescence imaging system (Fig. 6.18).

6.4.5 Ultrasonography (US) and Opt-acoustic (Photoacoustic) Imaging

As ultrasonography is primarily a morphological imaging test, metastatic LNs are diagnosed based on the size and shape. Enlarged and round shaped LNs can be diagnosed as metastatic like CT and MRI tests although it is often difficult to distinguish inflamed LNs from metastatic ones. Generally speaking, the heterogeneity of interior signals would be more significant in metastatic LNs than inflamed ones. Some US devise can provide doppler images. On doppler images, perfusion of metastatic lesions is likely to be enhanced. In contrast-enhanced studies, metastatic LNs are often strongly enhanced.

Recently, opt-acoustic imaging, which is also called photoacoustic imaging, is used for the detection of metastatic lesions. When some agents that can enhance the photoacoustic effects are administered, metastatic lesions in LNs show strong signals. Zhang et al. [41] reported the possibility of ultrasound-guided photoacoustic imaging for the selective detection of EGFR-expressing breast cancer and lymph node metastases in the experiments using anti-EGFR antibody-conjugated gold nanorods (Fig. 6.19).

6.5 Nonclinical Imaging Studies for SN Mapping

Direct visualization of LN metastasis at early stage is not easy even when imaging scanners with high performance are used because LNs with early metastases is often as small as normal LNs.

SN biopsy is an alternative way to diagnose LN metastases at the early stage. This procedure has been already performed for patients with early stage of breast cancer and malignant melanoma in routine clinical practice. Accurate identification of SNs is essential to successfully perform SN biopsy. In the clinical situation, two kinds of

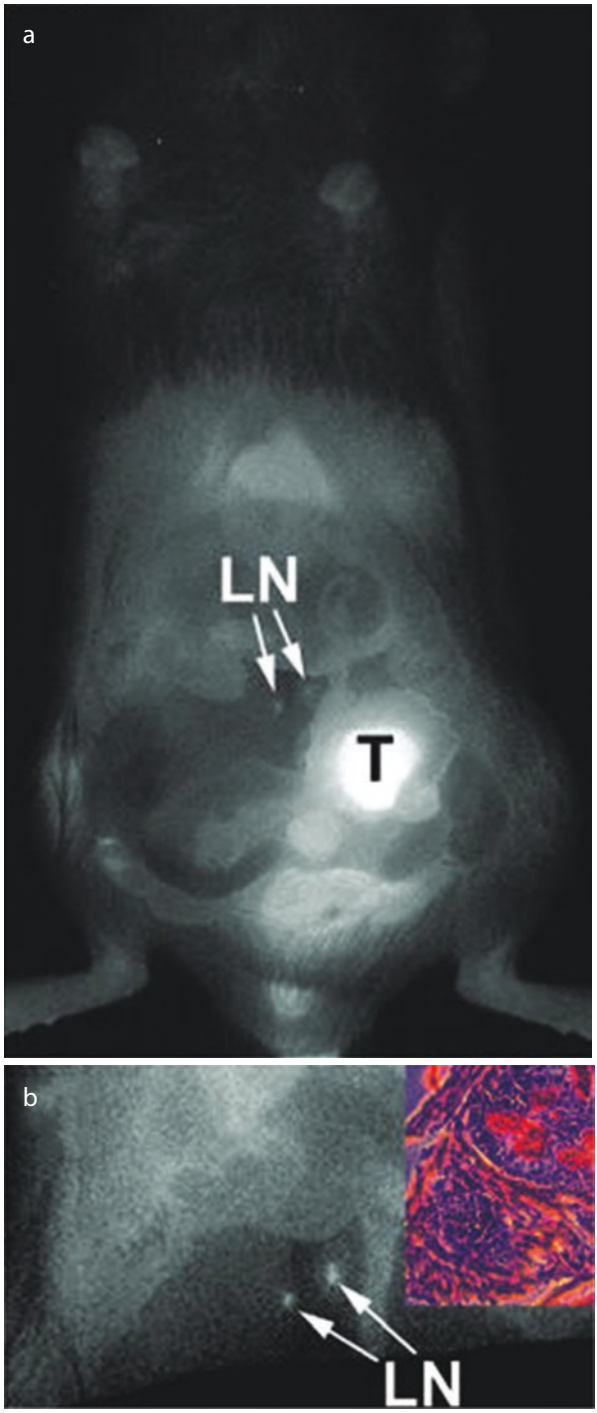

Fig. 6.17 Metastatic lesions including LN lesions in the mouse model visualized by the optical imaging using EGF conjugated with IRDye 800CW. Reprinted with some modification with permission from Ref. [40]

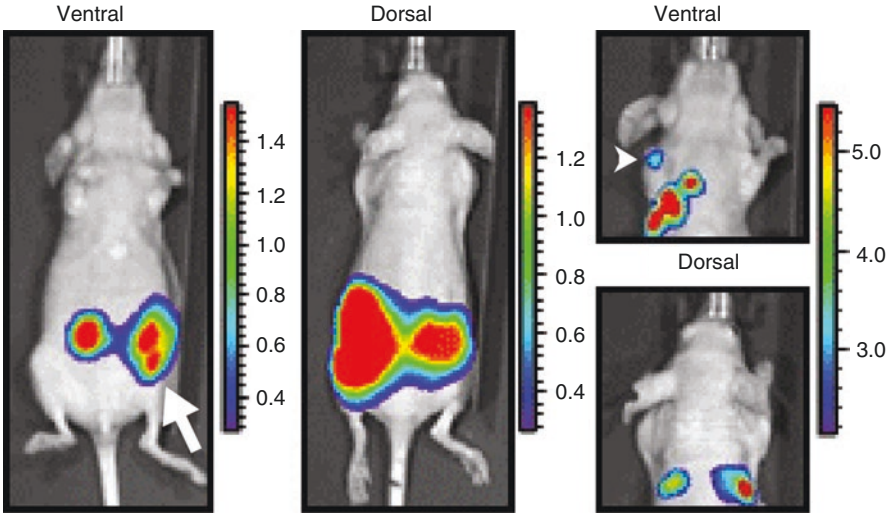

Fig. 6.18 An involved axillary LN (arrowhead) of an HT-29 orthotopic colorectal cancer (arrow) mouse model depicted by in vivo bioluminescence imaging. Reprinted with some modification with permission from Ref. [15]

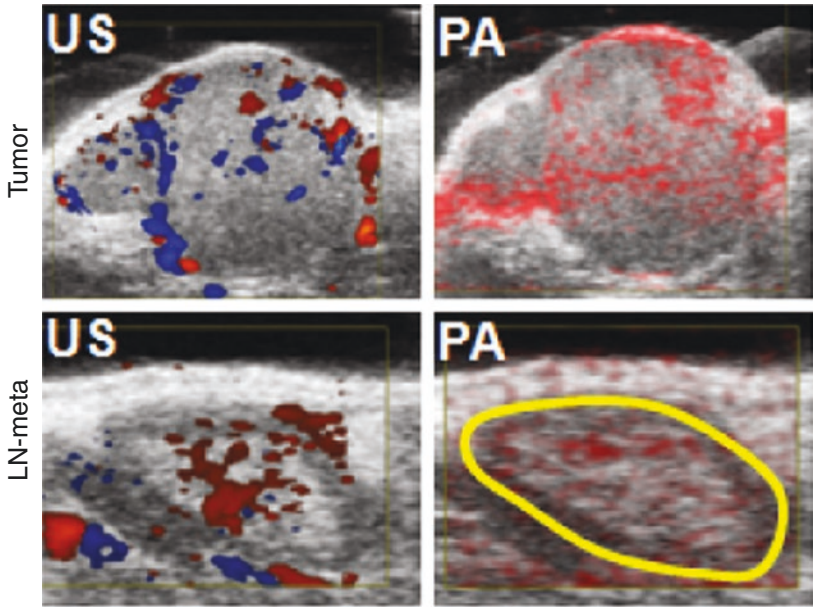

Fig. 6.19 The primary tumor and the metastatic LN in MDA-MB-231 orthotopic mouse xenograft model on the superimposed images of ultrasonography and acoustic imaging. Photoacoustic signal was enhanced by photo absorber (gold nanorods) conjugated antibodies. Reprinted with permission from Ref. [41]

lymphotropic agents are used for the detection of SNs: radiopharmaceuticals and optical imaging agents including blue dyes. In the preclinical investigation about SN mapping, these two kinds of new imaging agents are mainly under investigation.

6.5.1 Nonclinical Studies About Radiopharmaceuticals for SN Mapping

Most commonly used radiopharmaceuticals used in actual clinical SN mapping are radioactive colloids. In Japan, ^{99m}Tc-labeled phytate (FUJIFILM RI Pharma, Tokyo) and ^{99m}Tc-labeled tin colloids (Nihon Medi-physics, Nishinomiya) are covered by health insurance for SN mapping of breast cancer and malignant melanoma.

Regional LNs show high activity on SPECT images after ^{99m}Tc-labeled colloids are injected in animal models. For example, radiocolloids are injected in the mouse footpad, the popliteal LN shows high activity (Fig. 6.20).

These radioactive colloidal agents accumulate in SNs by phagocytosis of macrophages in SNs. Since molecular size of colloidal agents is large, most of injected colloidal agents stay at the injection site. This hinders the detection of SNs located near the injection site.

Therefore, new SN mapping agents with smaller molecular size are required. Although small molecules can easily move into lymphatic channels, they are likely to pass through SNs because they can be escaped from phagocytosis by macrophages. Therefore, SN seeking agents with small molecular size have to be trapped in SNs by some mechanisms. Mannose receptors on macrophages inside SNs can be good candidates to trap small molecular SN mapping agents. Vera et al. reported ^{99m}Tc-labeled tilmanocept that shows high affinity to these mannose receptors [42]. In Japan, Arano et al. [43] is also studying a new SN imaging agent that shows high affinity to mannose receptors on macrophages inside SNs. Nonclinical imaging tests are useful in the development of these new imaging agents. Arano's team demonstrated the clear visualization of SNs on SPECT tests in rat studies (Fig. 6.21).

These agents show good retention in SNs and they have potentials to clearly depict SNs located near the primary tumors since the molecular weight of these radioactive agents are small enough to wash out from the injection site.

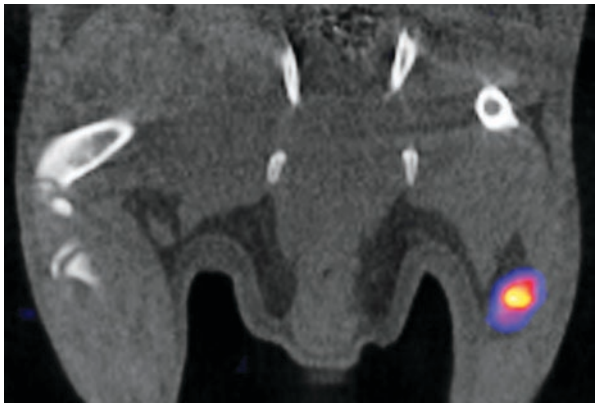

Fig. 6.20 A hot node in the popliteal region in ^{99m}Tc-labeled phytate SPECT/CT image. This hot node can be regarded as a SN of the left footpad lesion

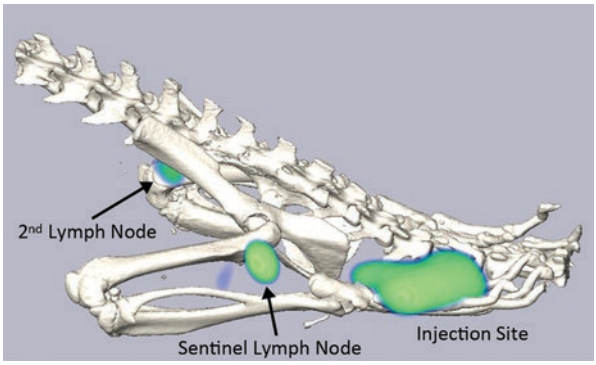

Fig. 6.21 The SN of a rat footpad visualized by the injection of ^{99m}Tc-labeled unique compounds with high affinity to mannose receptors on macrophages. By courtesy of Professor Yasushi Arano, Chiba University

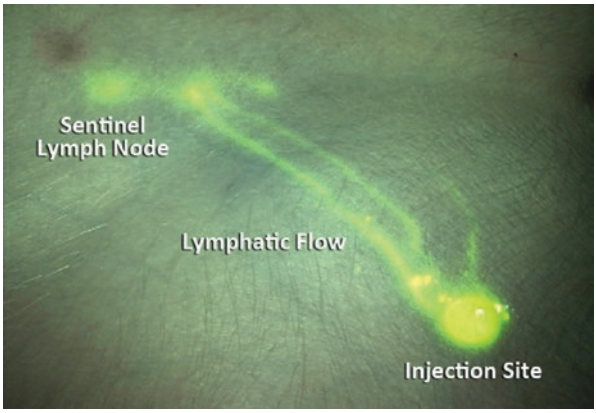

Fig. 6.22 The experimental SN mapping by quantum dots using a swine. Quantum dots can emit stronger fluorescent lights than that of ICG. By courtesy of Professor John V. Frangioni, Harvard Medical School

6.5.2 Nonclinical Studies About Optical Imaging Agents for SN Mapping

Optical methods are also important to identify SNs. Blue dyes are traditional optical imaging agents. In Japan, two kinds of blue dyes, ICG and Indigo carmine (Daiichi-Sankyo, Tokyo), are covered by health insurance for SN mapping of breast cancer and malignant melanoma.

As mentioned above, optical imaging with near-infrared lights is recently attracting interests of researchers. Since ICG emits near-infrared fluorescent lights in addition to blue visible lights, this dye is now used in SN biopsy under near-infrared light because optical imaging with near-infrared lights can visualize imaging agents with good contrast to low background signal.

As quantum dots can emit much stronger near-infrared fluorescent lights than ICG, they would be useful if they could be used in the clinical situation [44] (Fig. 6.22).

But, no quantum dots are approved for clinical use because of the toxicity issues due to heavy metals included in these agents.

Recently, optical imaging using near-infrared lights whose wave length is longer than 1000 nm (OTN-NIR lights) is spotlighted. An imaging scanner with InGaAs detectors and organic imaging dyes are developed [45, 46].

Since OTN-NIR lights can penetrate thicker soft tissues and observe deeper areas in the body, compared with conventional NIR lights, clinical application of SN mapping by optical imaging with these lights will be examined after this.

The clinical application of opt-acoustic imaging, another new imaging method, is also actively investigated [47].

6.5.3 Nonclinical Studies About Multi-modality Imaging for SN Mapping

In clinical SN mapping, it is reported that dual modality methods can yield the best performance, compared with radionuclides or optical agents alone.

Some dual modality imaging probes are reported in western countries. In Europe, the cocktails of ICG and ^{99m}Tc-labeled colloidal albumin are examined in mouse xenograft model [48].

Recently, Araki and our group [49] found that the cocktail of ICG and phytate showed good performance to detect SNs. When this cocktail was injected to mouse models, near-infrared fluorescence slowly appeared in SNs and this fluorescence continued for more than 1 day. This long fluorescent activity is suitable for the operation on head and neck regions. When phytate is labeled by ^{99m}Tc, the obtained radioactive ICG is expected to be useful to dual-modal detection of SNs. Since both of ICG and ^{99m}Tc-pytate are covered by health insurance in Japan, the clinical application of this unique cocktail would be feasible.

As for the evaluation of these dual-modality probes, fusion of two kinds of images is useful. Recently, as three-dimensional reconstruction method of optical images is proposed [50], information of optical images can be superimposed on tomographic scintigrams (Fig. 6.23).

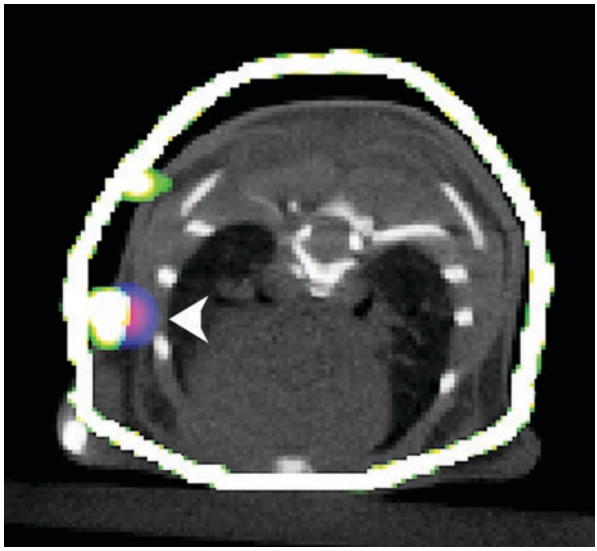

Fig. 6.23 The SN of a mouse forepaw (arrowhead) in optical and radionuclide fusion image. Three-dimensionally reconstructed optical images using ICG were superimposed on SPECT images with ^{99m}Tc-pytate after the injection of the cocktail of these two kinds of imaging agents

6.6 Indirect Visualization of Metastases in SNs

Although SN mapping is a useful method to detect LNs that are likely to have metastases, it is difficult to directly diagnose metastatic lesions only by SN mapping.

Since metastatic foci in SNs are usually small, most parts of interiors of SNs are occupied by non-tumor tissues. The evaluation of signals of these non-tumor tissues in SNs has a potential to detect metastatic lesions in SNs.

6.6.1 Visualization of Metastases in SNs by Negative Contrast Enhancement

Modifying signals of non-tumor tissues in SNs to enhance the contrast between metastatic foci and non-tumor areas can be alternative way to depict metastatic lesions in SNs. As described in the previous section, there are many macrophages in SNs and macrophages show strong phagocytic activity. When superparamagnetic iron oxide-based colloids are administered as contrast media of MRI, macrophages located in non-tumor areas in LNs phagocytose them and non-tumor areas are negatively enhanced, that is these areas show significant low signal, on T2*WI (When images are acquired using gradient echo sequences, T2*WIs were obtained instead of T2WIs).

Harisinghani et al. [51] reported small tumor lesions in LNs could be successfully diagnosed by this method in patients with prostatic cancer. Tatsumi et al. [52] reported that this strategy is also useful to diagnose LN metastases in gastric cancer.

But, some follow-up reports including our experimental study [53] revealed that inflammatory process or fat deposition could be false-positive findings (Fig. 6.24).

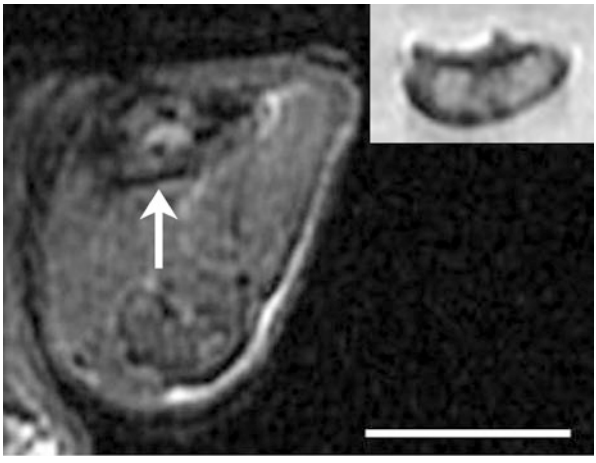

Fig. 6.24 An inflammatory swollen LN in the T2-star weighted MR image obtained after the injection of superparamagnetic iron oxide-based colloids. This non-tumor bearing LN looks like metastatic one. Reprinted with some modification with permission from Ref. [53]

6.6.2 Surrogate Imaging Based on Immune Response in Metastatic SNs

There are many immune cells in SNs besides macrophages and various kinds of immune reactions occur when SNs are involved by tumors. Although most researches have focused on the behavior of T cells, especially CD8+ T cells (CTL), B cells also react to metastatic lesions in SNs.

B cells are mainly located in superficial areas of LNs and these areas are called B-cell areas. When tumor antigens flow in LNs through afferent lymphatic channels, B cells interact with antigen-presenting cells and form follicles. Then, germinal centers appear in follicles.

We recently studied the interval changes of numbers of immune cells inside SNs by flow cytometry using C57BL/6 mice inoculated with B16 melanoma B cells and BALB/c mice with mouse breast cancer cells. Localization of these immune cells inside SNs was also longitudinally observed by immunohistochemistry.

Flow cytometry analyses revealed that, when compared to the control, the relative growth ratio of CD19-positive cells (B cells) increased more significantly than that of CD3-positive cells (T cells) according to the progression of metastases inside SNs. Immunohistochemical findings demonstrated the formation of germinal centers inside SNs was facilitated by advances of metastases (Fig. 6.25).

In the light of diagnostic imaging tests, more attention should be paid to cell groups that show more dramatic change in numbers according to the progress of metastases. We think that significant increase of the B cells and the formation of germinal centers inside SNs according to the progress of metastases would be good candidates for surrogate imaging biomarkers of metastases in SNs.

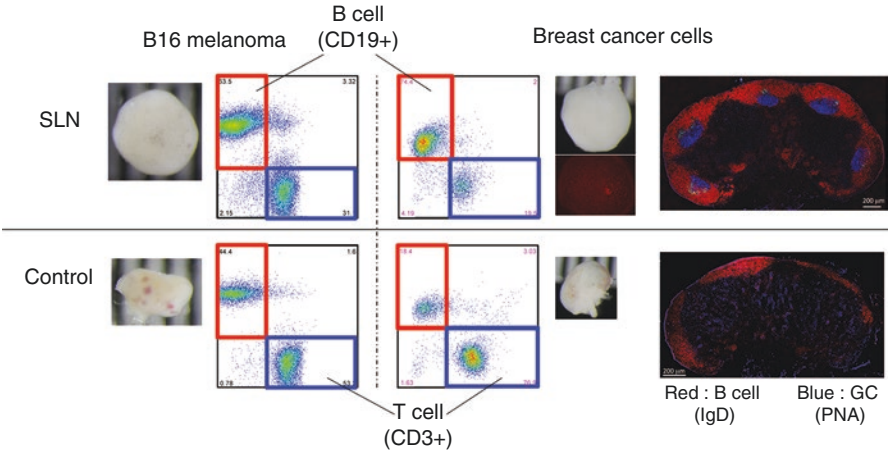

Fig. 6.25 Lymphocytes in the SN. The flow cytometry analyses showed that the B-cell (CD19+)/T-cell (CD3+) ratio in SNs increased compared to that in control nodes. Immunohistochemical analysis of SNs showed abundant germinal centers organized by lymphocytes with the expression of B-cell markers

Recently, Li et al. reported that ^{99m}Tc-labeled rituximab was useful to visualize SNs of patients with breast cancer [54]. Since rituximab is the monoclonal antibody drug that shows high affinity to CD20 antigen on B cells, it is considered that CD20-positive B cells increase in SNs of patients with breast cancer and these increased B cells are successfully detected by ^{99m}Tc-labeled rituximab on scintigrams.

As CD19 is an antigen that appears on B cells, like CD20, radioactive anti-CD19 antibodies have potential to evaluate the metastatic status of SNs. Since rituximab has been already approved as a drug to treat CD20-positive malignant lymphoma, anti-CD19 antibodies would be clinically applicable.

6.7 Summary and Key Points

In this chapter, we explained nonclinical imaging study to investigate LN metastases.

In the research of LN metastases, animal experiments are essential like other biomedical researches. The application of imaging tests is very useful because imaging tests can yield reliable and meaningful results at the sacrifice of minimal number of animals. But, the design of animal experiments must be carefully considered to obtain the fruitful results.

The followings are key points to achieve the aim of the study.

- The optimal animal models must be chosen considering the aim of researches although various kinds of animal models are now available.
- The most suitable imaging modality should be used although many different imaging scanners have been developed. Recently, combined scanners of different imaging modalities are getting popular such as PET/CT scanners. These combined scanners can provide more information that the simple summation of that is acquired from each scanner. Imaging devices dedicated for small animal imaging have been also developed, which show excellent spatial resolution and good sensitivity that are suitable for small animal imaging although these devices can image only small size of objects.
- Alternative imaging strategy should be considered in the detection of metastatic foci in LNs. Although direct visualization of metastatic lesions in LNs is ideal, small metastatic lesions in LNs are often difficult to visualize by current in vivo imaging technology. SN mapping is useful to identify LNs that are most likely to be invaded by tumors. The evaluation of signals of non-tumor areas in LNs would be a new strategy to diagnose small metastases in LNs because most parts of interiors of LNs are occupied by non-tumor tissues when metastatic lesions are small.

Since LN metastases are most important prognostic factors of gastrointestinal cancer, it is expected that accurate and reliable diagnostic criteria in in vivo diagnostic imaging tests will be established based on the valuable results induced by nonclinical animal imaging experiments.

References

1. Zitvogel L, Pitt JM, Daillere R, Smyth MJ, Kroemer G. Mouse models in oncoimmunology. Nat Rev Cancer. 2016;16(12):759–73. https://doi.org/10.1038/nrc.2016.91.
2. Lewis JS, Achilefu S, Garbow JR, Laforest R, Welch MJ. Small animal imaging: current technology and perspectives for oncological imaging. Eur J Cancer. 2002;38(16):2173–88. https://doi.org/10.1016/S0959-8049(02)00394-5.
3. Eckhardt BL, Francis PA, Parker BS, Anderson RL. Strategies for the discovery and development of therapies for metastatic breast cancer. Nat Rev Drug Discov. 2012;11(6):479–97. https://doi.org/10.1038/nrd2372.
4. Terracina KP, Aoyagi T, Huang W-C, Nagahashi M, Yamada A, Aoki K, et al. Development of a metastatic murine colon cancer model. J Surg Res. 2015;199(1):106–14. https://doi.org/10.1016/j.jss.2015.04.030.
5. Partecke LI, Sendler M, Kaeding A, Weiss FU, Mayerle J, Dummer A, et al. A syngeneic Orthotopic murine model of pancreatic adenocarcinoma in the C57/BL6 mouse using the Panc02 and 6606PDA cell lines. Eur Surg Res. 2011;47(2):98–107. https://doi.org/10.1159/000329413.
6. Jiang YJ, Lee CL, Wang Q, Zhou ZW, Yang F, Jin C, et al. Establishment of an orthotopic pancreatic cancer mouse model: cells suspended and injected in Matrigel. World J Gastroenterol. 2014;20(28):9476–85. https://doi.org/10.3748/wjg.v20.i28.9476.
7. Yang H, Kim C, Kim MJ, Schwendener RA, Alitalo K, Heston W, et al. Soluble vascular endothelial growth factor receptor-3 suppresses lymphangiogenesis and lymphatic metastasis in bladder cancer. Mol Cancer. 2011;10:36. https://doi.org/10.1186/1476-4598-10-36.
8. Aslakson CJ, Miller FR. Selective events in the metastatic process defined by analysis of the sequential dissemination of subpopulations of a mouse mammary-tumor. Cancer Res. 1992;52(6):1399–405.
9. Jeong HS, Jones D, Liao S, Wattson DA, Cui CH, Duda DG, et al. Investigation of the lack of angiogenesis in the formation of lymph node metastases. J Natl Cancer I. 2015;107(9):djv155. https://doi.org/10.1093/jnci/djv155.
10. Fidler IJ. Biological behavior of malignant melanoma cells correlated to their survival in vivo. Cancer Res. 1975;35(1):218–24.
11. Partridge SC, Kurland BF, Liu CL, Ho RJ, Ruddell A. Tumor-induced lymph node alterations detected by MRI lymphography using gadolinium nanoparticles. Sci Rep. 2015;5:15641. https://doi.org/10.1038/srep15641.
12. Zhu B, Lu L, Cai W, Yang X, Li C, Yang Z, et al. Kallikrein-binding protein inhibits growth of gastric carcinoma by reducing vascular endothelial growth factor production and angiogenesis. Mol Cancer Ther. 2007;6(12 Pt 1):3297–306. https://doi.org/10.1158/1535-7163.MCT-06-0798.
13. Fujihara T, Sawada T, Hirakawa K, Chung YS, Yashiro M, Inoue T, Sowa M. Establishment of lymph node metastatic model for human gastric cancer in nude mice and analysis of factors associated with metastasis. Clin Exp Metastasis. 1998;16(4):389–98.
14. Yanagihara K, Takigahira M, Tanaka H, Komatsu T, Fukumoto H, Koizumi F, et al. Development and biological analysis of peritoneal metastasis mouse models for human scirrhous stomach cancer. Cancer Sci. 2005;96(6):323–32. https://doi.org/10.1111/j.1349-7006.2005.00054.x.
15. Fernández Y, Foradada L, García-Aranda N, Mancilla S, Suárez-López L, Céspedes MV, Herance JR, Arango D, Mangues R, Schwartz S Jr, Abasolo I. Bioluminescent imaging of animal models for human colorectal cancer tumor growth and metastatic dissemination to clinically significant sites. J Mol Biol Mol Imaging. 2015;2:2.
16. Hackl C, Man S, Francia G, Milsom C, Xu P, Kerbel RS. Metronomic oral topotecan prolongs survival and reduces liver metastasis in improved preclinical orthotopic and adjuvant therapy colon cancer models. Gut. 2013;62(2):259–71. https://doi.org/10.1136/gutjnl-2011-301585.

17. Bhullar JS, Subhas G, Silberberg B, Tilak J, Andrus L, Decker M, et al. A novel nonoperative Orthotopic colorectal Cancer murine model using electrocoagulation. J Am Coll Surg. 2011;213(1):54–60. https://doi.org/10.1016/j.jamcollsurg.2011.02.022.
18. Gros SJ, Dohrmann T, Peldschus K, Schurr PG, Kaifi JT, Kalinina T, et al. Complementary use of fluorescence and magnetic resonance imaging of metastatic esophageal cancer in a novel orthotopic mouse model. Int J Cancer. 2010;126(11):2671–81. https://doi.org/10.1002/ijc.24980.
19. Le CP, Nowell CJ, Kim-Fuchs C, Botteri E, Hiller JG, Ismail H, et al. Chronic stress in mice remodels lymph vasculature to promote tumour cell dissemination. Nat Commun. 2016;7:10634. https://doi.org/10.1038/ncomms10634.
20. Nagata H, Arai T, Soejima Y, Suzuki H, Ishii H, Hibi T. Limited capability of regional lymph nodes to eradicate metastatic cancer cells. Cancer Res. 2004;64(22):8239–48. https://doi.org/10.1158/0008-5472.Can-04-1182.
21. Trencsenyi G, Marian T, Bako F, Emri M, Nagy G, Kertai P, et al. Metastatic hepatocarcinoma he/de tumor model in rat. J Cancer. 2014;5(7):548–58. https://doi.org/10.7150/jca.9315.
22. Tang L, Duan R, Zhong YJ, Firestone RA, Hong YP, Li JG, et al. Synthesis, identification and in vivo studies of tumor-targeting agent peptide doxorubicin (PDOX) to treat peritoneal carcinomatosis of gastric cancer with similar efficacy but reduced toxicity. Mol Cancer. 2014;13:44. https://doi.org/10.1186/1476-4598-13-44.
23. Shen N, Tan J, Wang P, Wang J, Shi Y, Lv W, et al. Indirect magnetic resonance imaging lymphography identifies lymph node metastasis in rabbit pyriform sinus VX2 carcinoma using ultra-small super-paramagnetic iron oxide. PLoS One. 2014;9(4):e94876. https://doi.org/10.1371/journal.pone.0094876.
24. Goldberg BB, Merton DA, Liu JB, Thakur M, Murphy GF, Needleman L, et al. Sentinel lymph nodes in a swine model with melanoma: contrast-enhanced lymphatic US. Radiology. 2004;230(3):727–34. https://doi.org/10.1148/radiol.2303021440.
25. Benezra M, Penate-Medina O, Zanzonico PB, Schaer D, Ow H, Burns A, et al. Multimodal silica nanoparticles are effective cancer-targeted probes in a model of human melanoma. J Clin Invest. 2011;121(7):2768–80. https://doi.org/10.1172/JCI45600.
26. Ito M, Hiramatsu H, Kobayashi K, Suzue K, Kawahata M, Hioki K, et al. NOD/SCID/gamma(null)(c) mouse: an excellent recipient mouse model for engraftment of human cells. Blood. 2002;100(9):3175–82. https://doi.org/10.1182/blood-2001-12-0207.
27. Shultz LD, Lyons BL, Burzenski LM, Gott B, Chen XH, Chaleff S, et al. Human lymphoid and myeloid cell development in NOD/LtSz-scid IL2R gamma(null) mice engrafted with mobilized human hemopoietic stem cells. J Immunol. 2005;174(10):6477–89.
28. de Jong M, Essers J, van Weerden WM. Imaging preclinical tumour models: improving translational power. Nat Rev Cancer. 2014;14(7):481–93. https://doi.org/10.1038/nrc3751.
29. Wiig H, Swartz MA. Interstitial fluid and lymph formation and transport: physiological regulation and roles in inflammation and cancer. Physiol Rev. 2012;92(3):1005–60. https://doi.org/10.1152/physrev.00037.2011.
30. Trevaskis NL, Kaminskas LM, Porter CJ. From sewer to saviour – targeting the lymphatic system to promote drug exposure and activity. Nat Rev Drug Discov. 2015;14(11):781–803. https://doi.org/10.1038/nrd4608.
31. Fujii H, Umeda IO, Kojima Y. Instruments for radiation measurement in life sciences (5). 'Development of imaging technology in life sciences'. 8. Small animal imaging using SPECT. Radioisotopes (Tokyo). 2008;57(3):219–32.
32. Mitsuda M, Yamaguchi M, Furuta T, Nabetani A, Hirayama A, Nozaki A, et al. Multiple-animal MR imaging using a 3T clinical scanner and multi-channel coil for volumetric analysis in a mouse tumor model. Magn Reson Med Sci. 2011;10(4):229–37.
33. James ML, Gambhir SS. A molecular imaging primer: modalities, imaging agents, and applications. Physiol Rev. 2012;92(2):897–965. https://doi.org/10.1152/physrev.00049.2010.
34. Walk EL, McLaughlin SL, Weed SA. High-frequency ultrasound imaging of mouse cervical lymph nodes. J Vis Exp. 2015;101:e52718. https://doi.org/10.3791/52718.

35. Bell AG. LXVIII. Upon the production of sound by radiant energy. London Edinburgh Dublin Philos Mag J Sci. 1881;11(71):510–28.
36. Mehrmohammadi M, Yoon SJ, Yeager D, Emelianov SY. Photoacoustic imaging for cancer detection and staging. Curr Mol Imaging. 2013;2(1):89–105. https://doi.org/10.2174/2211555211302010010.
37. Dorfman RE, Alpern MB, Gross BH, Sandler MA. Upper abdominal lymph-nodes – criteria for normal size determined with Ct. Radiology. 1991;180(2):319–22.
38. Duncan K, Rosean TR, Tompkins VS, Olivier A, Sompallae R, Zhan F, et al. (18)F-FDG-PET/CT imaging in an IL-6- and MYC-driven mouse model of human multiple myeloma affords objective evaluation of plasma cell tumor progression and therapeutic response to the proteasome inhibitor ixazomib. Blood Cancer J. 2013;3:e165. https://doi.org/10.1038/bcj.2013.61.
39. Mumprecht V, Honer M, Vigl B, Proulx ST, Trachsel E, Kaspar M, et al. In vivo imaging of inflammation- and tumor-induced lymph node lymphangiogenesis by immuno-positron emission tomography. Cancer Res. 2010;70(21):8842–51. https://doi.org/10.1158/0008-5472.Can-10-0896.
40. Kovar JL, Johnson MA, Volcheck WM, Chen J, Simpson MA. Hyaluronidase expression induces prostate tumor metastasis in an orthotopic mouse model. Am J Pathol. 2006;169(4):1415–26. https://doi.org/10.2353/ajpath.2006.060324.
41. Zhang MH, Kim HS, Jin TF, Yi A, Moon WK. Ultrasound-guided photoacoustic imaging for the selective detection of EGFR-expressing breast cancer and lymph node metastases. Biomed Opt Express. 2016;7(5):1920–31. https://doi.org/10.1364/Boe.7.001920.
42. Vera DR, Wallace AM, Hoh CK, Mattrey RF. A synthetic macromolecule for sentinel node detection: Tc-99m-DTPA-mannosyl-dextran. J Nucl Med. 2001;42(6):951–9.
43. Takagi K, Uehara T, Kaneko E, Nakayama M, Koizumi M, Endo K, et al. 99mTc-labeled mannosyl-neoglycoalbumin for sentinel lymph node identification. Nucl Med Biol. 2004;31(7):893–900. https://doi.org/10.1016/j.nucmedbio.2004.04.008.
44. Kim S, Lim YT, Soltesz EG, De Grand AM, Lee J, Nakayama A, et al. Near-infrared fluorescent type II quantum dots for sentinel lymph node mapping. Nat Biotechnol. 2004;22(1):93–7. https://doi.org/10.1038/nbt920.
45. Jaque D, Richard C, Viana B, Soga K, Liu X, García SJ. Inorganic nanoparticles for optical bioimaging. Adv Opt Photon. 2016;8(1):1. https://doi.org/10.1364/aop.8.000001.
46. Antaris AL, Chen H, Cheng K, Sun Y, Hong GS, Qu CR, et al. A small-molecule dye for NIR-II imaging. Nat Mater. 2016;15(2):235. https://doi.org/10.1038/Nmat4476.
47. Luke GP, Myers JN, Emelianov SY, Sokolov KV. Sentinel lymph node biopsy revisited: ultrasound-guided photoacoustic detection of micrometastases using molecularly targeted plasmonic nanosensors. Cancer Res. 2014;74(19):5397–408. https://doi.org/10.1158/0008-5472.Can-14-0796.
48. van Leeuwen AC, Buckle T, Bendle G, Vermeeren L, Olmos RV, van de Poel HG, et al. Tracer-cocktail injections for combined pre- and intraoperative multimodal imaging of lymph nodes in a spontaneous mouse prostate tumor model. J Biomed Opt. 2011;16(1):016004. https://doi.org/10.1117/1.3528027.
49. Araki K, Mizokami D, Tomifuji M, Yamashita T, Ohnuki K, Umeda IO, et al. Novel indocyanine green-phytate colloid technique for sentinel node detection in head and neck: mouse study. Otolaryngol Head Neck Surg. 2014;151(2):279–85. https://doi.org/10.1177/0194599814530409.
50. Okawa S, Ikehara T, Oda I, Yamada Y. Reconstruction of localized fluorescent target from multi-view continuous-wave surface images of small animal with lp sparsity regularization. Biomed Opt Express. 2014;5(6):1839–60. https://doi.org/10.1364/BOE.5.001839.
51. Harisinghani MG, Barentsz J, Hahn PF, Deserno WM, Tabatabaei S, van de Kaa CH, et al. Noninvasive detection of clinically occult lymph-node metastases in prostate cancer. New Engl J Med. 2003;348(25):2491–U5. https://doi.org/10.1056/NEJMoa022749.
52. Tatsumi Y, Tanigawa N, Nishimura H, Nomura E, Mabuchi H, Matsuki M, et al. Preoperative diagnosis of lymph node metastases in gastric cancer by magnetic resonance imaging with ferumoxtran-10. Gastric Cancer. 2006;9(2):120–8. https://doi.org/10.1007/s10120-006-0365-8.

53. Suzuki D, Yamaguchi M, Furuta T, Okuyama Y, Yoshikawa K, Fujii H. Central high signal in inflammatory swollen lymph nodes on SPIO-enhanced interstitial MR lymphograms: a mimic of lymph node metastasis. Magn Reson Med Sci. 2012;11(1):61–3.
54. Li N, Wang XJ, Lin BH, Zhu H, Liu C, Xu XB, et al. Clinical evaluation of Tc-99m-rituximab for sentinel lymph node mapping in breast cancer patients. J Nucl Med. 2016;57(8):1214–20. https://doi.org/10.2967/jnumed.115.160572.